

Desulfovibrio fairfieldensis adhesion on implantable titanium used in odontology: a preliminary study

Alex Tchinda, Gaël Pierson, Laetitia Chezeau, Richard Kouitat-Njiwa, Bertrand Henri Rihn, Pierre Bravetti*

Université de Lorraine, CNRS, Institut Jean Lamour, F-54000 Nancy, France

*Correspondence to: pierre.bravetti@univ-lorraine.fr

Received April 13, 2021; Accepted July 6, 2021; Published August 31, 2021

Doi: <http://dx.doi.org/10.14715/cmb/2021.67.2.9>

Copyright: © 2021 by the C.M.B. Association. All rights reserved.

Abstract: the study presented here aimed to assess the ability of *Desulfovibrio fairfieldensis* bacteria to adhere to and form biofilm on the structure of titanium used in implants. *D. fairfieldensis* was found in the periodontal pockets in the oral environment, indicating that these bacteria can colonize the implant-bone interface and consequently cause bone infection and implant corrosion.

Plates of implantable titanium, of which surfaces were characterized by scanning electronic microscopy and Raman spectroscopy, were immersed in several suspensions of *D. fairfieldensis* cells containing potassium nitrate on the one hand, and artificial saliva or a sulfato-reducing bacterial culture medium on the other hand. Following various incubation timepoints bacteria were counted in different media to determine their doubling time and titanium samples are checked for and determination of the total number of adhered bacteria and biofilm formation.

Adhesion of *D. fairfieldensis* on titanium occurs at rates ranging from 2.10^5 to $4.6.10^6$ bacteria $h^{-1}cm^{-2}$ in the first 18 h of incubation on both native and implantable titanium samples. Following that time, the increase in cell numbers per h and cm^2 is attributed to growth in adhered bacteria. After 30 days of incubation in a nutrient-rich medium, dense biofilms are observed forming on the implant surface where bacteria became embedded in a layer of polymers

D. fairfieldensis is able of adhering to an implantable titanium surface in order to form a biofilm. Further studies are still necessary, however, to assess whether this adhesion still occurs in an environment containing saliva or serum proteins that may alter the implant surface.

Key words: *Desulfovibrio fairfieldensis*; Dental Implant; Titanium; Adhesion; Biofilm; Periodontitis; Biodegradation; Corrosion; Osseointegration.

Introduction

The dental implant we analyzed is a titanium artificial tooth root for implantation in the maxillary or mandibular bone to support a prosthetic element. Titanium is the most commonly used material in dental implants. Its excellent biocompatibility makes it an excellent choice for implant manufacturing (1). A layer of titanium oxide forms on the implant's surface once it is in place, a process called passivation. Titanium is very well tolerated by the body and has so far never been linked with a lack of osseointegration or allergies. Three to six months following implantation, bone cells attach to the titanium surface, leading to osseointegration, also termed bone healing (1, 2). This osseointegration causes vertical bone loss of 0.5 mm on average in the first year post-implantation, followed by a loss of 0.1 μm on average per year (3). The bone healing around the implant is slight, still fulfilling the criteria of clinical success. This osseointegration, however, can be hampered, causing implant failure, the main causes of which are excessive bone loss surrounding the implant and bacterial adhesion to the implant surface (3), which can be caused by the implantation procedure that did not ensure adequate asepsis. This failure then leads to artificial root mobility or infection.

Moreover, despite its high corrosion resistance, tita-

nium is affected by the aggressive environment of the mouth, particularly featuring electrolytes of the saliva, that progressively induce biodegradation by oxidation and solubilization of the upper metal layer. This passivation layer on the titanium could thus be altered in these conditions, consequently causing corrosion of the metal (4, 5). This corrosion can be considerably accelerated following bacterial colonization, at which point it is termed 'biocorrosion' or microbial-influenced corrosion.

The topography of dental implants in the mouth appears to allow bacteria access to the dental implant surface. We know that peri-implant soft tissues do not adhere as effectively to implants as the gingiva tissues do to teeth. No epithelial adhesion occurs using hemidesmosomes, nor is there any connective tissue attachment to implants. Only pseudopods of junctional epithelium adhere to implant surfaces, creating a fragile permeable barrier through which bacteria can penetrate and colonize dental implants and further bone (Figure 1). This colonization can lead to corrosive damage of the implant, destabilizing it and potentially causing disease relating to microbial infection. In implant-induced periodontitis, bacteria reach the implant surface then adheres to its surface allowing a biofilm to form. This can lead to peri-implantitis that is difficult to treat, and could additionally cause the titanium implant to deteriorate

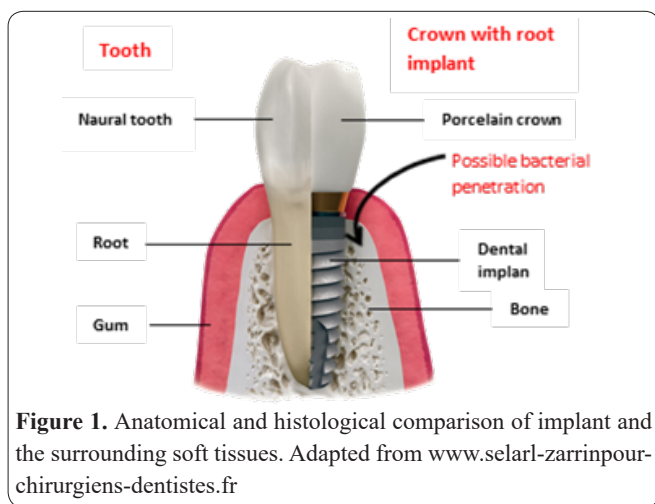


Figure 1. Anatomical and histological comparison of implant and the surrounding soft tissues. Adapted from www.selarl-zarrinpour-chirurgiens-dentistes.fr

over time due to biocorrosion (6). The challenge posed in treating this type of infection is, on the one hand, due to the absence of epithelial or connective tissue attachment, and on the other because of the growth of bacteria in the form of a biofilm. Both factors prevent antibiotics from reaching their target effectively. For non-induced by implant periodontitis, common treatment involves surgical subgingival scaling of bacterial tartar followed by a week of antibiotic medical treatment.

Sulfate-reducing bacteria of the *Desulfovibrio* genus are strongly suspected of being at the heart of these complications. These are Gram-negative bacteria, straight or curved, non-sporing, with obligate anaerobic mechanism, using sulfates or other sulfate compounds (*e.g.* thiosulfates) as terminal electron acceptors in their respiratory chain (7, 8). In the periodontal pockets, where they are already isolated (9, 10), the production of H₂S from their sulfate-reducing activity has the particular effect of causing direct toxicity to the collagen fibers and indirect harm to the immunological defenses as described previously (11). Furthermore, many of these strains have been reported to cause infection (7). These bacteria are also well-known in many different fields for their corrosive power (12).

From studying the 16S rDNA, we know that the *Desulfovibrio* genus is related to the *Bilophila* and *Lawsonia* genera. These three types form the *Desulfovibrionales* family (class: *Deltaproteobacteria*, phylum of “proteobacteria”, of the *Eubacteriaceae* family, Figure 2). The habitat of *Desulfovibrio* is large, with species found in sediments, polluted rivers and lakes, sewage and purification systems like anaerobic digesters and reed-bed systems, hydromorphic soils, sea and river port installations, oil pipelines, water systems (such as cooling systems, some constructed with titanium, or drinking water networks, etc.), and nuclear power plant heat

exchangers (6, 13-15). They have also been found in the digestive tract, lung, brain, and liver abscesses either in humans or in animals, as well as in human blood (8-10, 16). In humans, at least four different species of *Desulfovibrio* have been reported of which *fairfieldensis*, *piger*, and *vulgaris* (17, 8). Diagnosing *Desulfovibrio sp.* Infection remains challenging due to these bacteria’s specific nutritional demand in laboratory conditions, as well as 16S rDNA sequencing-based identification methods still being rare in medical diagnosis.

The *BBL Crystal anaerobe identification system*™ assay (Becton Dickinson) enables identification of genera, but not of different species that was performed by Rapide ANA II system (Remed), Viteck AN I card (bioMérieux), and API 20A (bioMérieux) bioassays. Warren *et al.* (8) proposed an identification method capable of characterizing the different *Desulfovibrio sp.* Strains found in humans and differentiating them from similar bacteria. This identification process is outlined in Table I.

As evidenced in Table I, *Desulfovibrio sp.* Bacteria

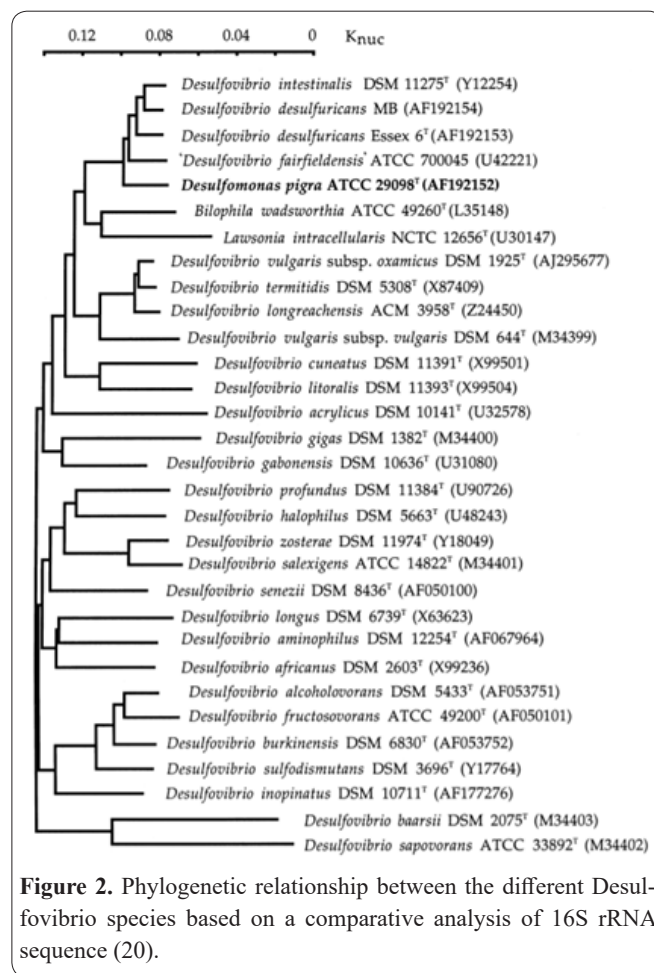


Figure 2. Phylogenetic relationship between the different *Desulfovibrio* species based on a comparative analysis of 16S rRNA sequence (20).

Table 1. Biochemical identification of species of *Desulfovibrio* genus (5) (S= sensitive, or R = resistant to antibiotics. Numbers indicate the percentages of strains generating positive responses after 24 h.

Species	1	2	3	4	5	6	7	8	9	10	11
<i>Desulfovibrio piger</i>	S	R	R	0	0	0	100	0	0	0	100
<i>Desulfovibrio fairfieldensis</i>	S	R	R	100	0	100	100	0	0	100	100
<i>Desulfovibrio desulfuricans</i>	S	R	R	0	0	100	0	100	100	100	100
<i>Desulfovibrio vulgaris</i>	S	R	R	0	100	0	100	0	0	100	100

1) Kanamycin (1 mg) 2) Vancomycin (5 µg); 3) Colistine (10 µg); 4) Indole; 6) Nitrate reductase; 7) Growth in presence of bile; 8) Urease; 9) Motility 10) Presence of desulfovibrindine; 11) production hydrogen sulfide in SIM (sulfide-indole-motility) medium (8).

are sensitive to metronidazole and chloramphenicol, and nearly always present sensitivity to imipenem and clindamycin. Most strains are, however, resistant to penicillin. The most resistant strain appears to be *Desulfovibrio fairfieldensis* (8). This strain, suspected of being one of the major sulfate-reducing bacteria (SRB) that colonize periodontal pockets, resembles any typical *Desulfovibrio* bacterium, being either straight or curved with a diameter of 0.5 to 1 μm and length of 2.5 to 5 μm and can feature a polar flagellum (Figure 2). In odontology, this strain holds particular interest as it was recently found colonizing periodontal pockets in humans (9, 10, 16) and is known for causing pathogens thought to be specific to humans (10, 18, 19).

The adhesive properties of these bacteria, combined with their capacity to form biofilm on titanium implants, could explain the infections they cause and why they are found in the periodontal space. Still, there are very little data available on this species, or on many other bacteria of this genus to that matter, regarding their behavior with titanium-designed implants. Incubation of *D. vulgaris* at room temperature (RT) for 90 d with polished titanium surfaces reported biodegradation evidenced by pit formation and surface corrosion (6). Same modifications of stainless steel and on an alloy composed of stainless steel and nickel was induced by their incubation for *D. desulfuricans* at 37°C and *D. desulfuricans* at 26°C respectively (21, 22).

Contrarily with the previously mentioned studies, we used etched or sandblasted titanium in order to reproduce the conditions, in terms of surface quality, of 'real' implants. Following culture in complete cell culture medium, we incubated *D. fairfieldensis* cultures in stationary growth phase either in nutrient-free medium to evaluate their adhesion rate or in artificial saliva (AS) to mimic conditions of the human mouth. Similar experiments were performed in parallel with a strain of *D. desulfuricans* as a control.

As bacterium adhesion to implant and ability to form biofilm could be the cause of their invasive colonization of the bone/dental implant interface, our study rationale was (i) to assess the adhesion ability of *D. fairfieldensis* and (ii) to evidence the formation of biofilm on the surface of dental implants of titanium in vitro as no adhesion study has been performed on titanium incubated with *D. fairfieldensis* as far as our knowledge.

Materials and Methods

Solid titanium

Rectangular plates of solid titanium were cut in 1 cm x 1 cm x 1 mm, giving a total unfolded area of 2.4 cm². Those specimens were heated to 550°C for 2 h to remove all traces of organic matter.

Implantable titanium

Circular plates of grade 4 titanium, commercial-grade pure titanium and measuring 5 mm in diameter by 1 mm thickness, namely an unfolded area of 0.5498 cm², were purchased at Straumann (Basel, Switzerland). The specimens had been sterilized by gamma irradiation and stored under double-layer wrapping by the manufacturer. The quality of the surface of those samples was the same as those of implants ready for insertion in bone,

i.e., SLA[®] quality. This means the surface was macro- and microstructured to ensure faster and more efficient osseointegration. SLA[®] surface quality involves sandblasting with corundum particles followed by HCl/H₂SO₄ acid treatment at high temperature for several min. This process causes roughness composed of small pits measuring 2 to 4 μm of depth.

Characterization of specimen surfaces

The surface quality of the two specimen types was characterized using Scanning Electron Microscopy (A. Kohler, of the School of Medicine core facility, Nancy, France). Raman spectroscopy allowed surface chemical characterization of implantable titanium specimens performed as described previously (23). Raman spectra were recorded in triple subtractive mode using a multi-channel CDD detector (Jobin-Yvon Raman T64000[®], Nancy, France). using liquid nitrogen for cooling and a 514 nm argon laser source for excitation. The Raman scattering signal was registered at 180° via a confocal microscope equipped with a 100 magnitude lens and a numerical aperture of 0.95. Both theoretical lateral and axial spatial resolutions were respectively of 0.24 and 0.78 μm

Culture and characterization of *D. fairfieldensis* and *D. desulfuricans* strains

Immediately on arrival in lyophilized form, the strains of *D. fairfieldensis* (ATCC # 700045, a generous gift of D Raoult, Rickettsies unit, Marseilles, France) and *D. desulfuricans* DSMZ (Deutsche Sammlung von Mikroorganismen und Zellkulturen) # 642 were rehydrated in 0.5 mL of DSMZ medium. Once hydrated, the bacteria were cultivated on *Columbia blood agar* then incubated in an anaerobic box (Coy Chamber, USA) under an N₂/H₂ (98/2 v/v) atmosphere at 30°C \pm 2°C. The strains were kept in a mixture of mixture glycerol/growth medium (15/85 v/v) at -80° C. After 4 d of incubation, small translucent colonies typical of the genus were visible (data not shown). After a 7-d incubation period, a subculture was performed on CBA for bacterial identification. Bacteria were subcultured every week in DSMZ medium in 4 100-mL sterile glass vials, hermetically sealed by a butyl stopper and recovered of an aluminum cap and maintained at 37°C.

Bacteria enumeration

The total number of bacteria was determined by fluorochrome labeling (DAPI: 4', 6-diamidino-2-phenylindol, CAS 28718-90-3) to color bacterial DNA following UV excitation at 365 nm using an epifluorescence microscope (LCPME, Nancy, France). Bacteria in suspension are filtered using Millipore GTBP047000[®] polycarbonate membranes (0.22 μm , Molsheim, France), while adhered bacteria are counted directly on the titanium samples after labeling.

Bacteria in suspension

Bacteria cells in suspension (1 mL) were fixed in 2 % formaldehyde for 5 min then diluted to a 10th with sterile, nonpyrogenic water (B-Braun water, Melsungen, Germany). The solution was then diluted in four 20-mL tubes using 9 mL of non-pyrogenic water, to which 1 mL of Triton (0.1% m/v) then 1 mL of DAPI

were added (0.5 µg/mL final concentration). Following a fast homogenization by vortexing (5 s), serial dilutions of 1/10th were performed that are conserved for 15 min at RT in the dark until the filtration step.

The contents of each tube were vacuum filtered onto the same polycarbonate 0.22 µm membranes (using a flame-sterilized stainless steel Millipore filter manifold, (Molsheim France). Then the filter top units were rinsed in 5 mL non-pyrogenic water. The membrane filters were placed in individual Petri dishes and dried by blowing hot air. The filters were then mounted between slide and coverslip with one drop of glycerol for rehydration (Diagnostic Pasteur, 74921). Slides were analyzed by epifluorescence microscopy as described previously (Olympus, BX51) under ×100 magnification using non-fluorescent immersion oil. The total number of bacteria was expressed using the following formula: $N = (N'/V) \times (EFA / FA) \times D$ where N is the number of bacteria per mL, N' the number of bacteria per field (mean), V the filtered volume (mL), EFA the effective filtration area (9.81.10⁻⁴ m²), FA the field area (5.66.10⁻⁹ m²) and D the dilution factor.

Attached bacteria

Following incubation of titanium specimens in bacterial suspension, samples were removed in aseptic conditions, immersed twice for 30 s in a sterile buffer of 0.05 M KNO₃ in order to eliminate any bacteria not or slightly adhering to the surface. Bacteria were fixed in a solution of 0.05 M KNO₃ and 2 % formaldehyde for 5 min. Titanium specimens were then (i) rinsed twice in a solution of 0.05 M KNO₃, (ii) incubated in 0.5 µg/mL DAPI dye for 15 min in the dark at RT, (iii) rinsed once in KNO₃ buffer, (iv) dried and (v) finally mounted on a slide for optical microscopy as described previously. Observed fluorescent bacteria were all counted in 20 fields and the average number of adhered bacteria per cm² was calculated.

Incubation of specimens with bacterial suspensions

Columbia ablood agar isolated colonies were put in 50 mL of DSMZ or AS media for a 48-h culture period. Bacterial growth was recorded by measuring absorbance at 600 nm every 24 h over 8 d. Bacterial count on filtered solutions by DAPI labeling enabled us to correlate their absorbance (in Mac Farland units) and their absolute number. Thus 0.2 absorbance unit at 600 nm corresponded approximately to 6.7.10⁸ cells/mL.

Four vials containing DSMZ and 4 vials with AS medium were grown with *D. fairfieldensis*. At the end of the exponential growth phase (5 d), their content was centrifuged at 5000× g for 10 min and the pellet was recovered in N₂/H₂ (98/2 v/v) atmosphere where bacteria were washed twice by centrifugation in sterile 0.05 M KNO₃ buffer. Two new suspensions in 0.05 M KNO₃ or 100 mL AS buffer were adjusted for a 600 nm absorbance of 0.2 unit and their pH was measured.

We incubated 80 mL of those suspensions in 6 sterile glass Petri dishes containing 40 mL of: (i) bacterial suspension without titanium specimen (dish #1); (ii) bacterial suspension with five titanium specimens (dish #2); (iii) sterile KNO₃ at 0.05 M with 2 titanium specimens without bacteria (dish #3), (iv) bacterial suspension in AS buffer with five titanium specimens (dish #4), (v)

AS buffer without bacteria with two titanium specimens (dish #5) and (vi) AS buffer without titanium specimens (dish #6). Petri dishes were incubated in an anaerobic CoyTM chamber under N₂/H₂ (98/2) atmosphere at 30°C ± 2 for 4 d.

Preparation of specimens for SEM analysis

In order to assess the possible development of biofilm onto the titanium specimens, we incubated them for over 7 d with bacteria. To prevent evaporation in an anaerobic chamber long-term incubation at 37°C was achieved using 100 mL vials hermetically sealed with butyl stoppers (Bellco, Vineland, NJ).

Indeed each titanium specimen was stored for 30 d in a 100 mL vial containing 50 mL DSMZ culture medium, with or without bacteria. In order to provide sufficient nutrients, 2/3 of the culture medium was removed and replaced by fresh medium twice during the incubation period: after d 10 and d 20. For each timepoint, titanium specimens were removed for observation and were (i) immersed three times for one min in 0.05 M KNO₃ sterile buffer, (ii) fixed overnight in 0.1 M PBS buffer with 2.5 % glutaraldehyde pH = 7.2 and (iii) gradually dehydrated in ethanol/water (v/v) solutions for 2 min: 30%, 50%, 60%, 70%, 80%, 90%, and finally immersed in pure ethanol that was eliminated by two successive washes in hexamethyldisilazane. The specimens were then dried for 15 min and recovered with carbon black.

Results

Characterization of titanium specimen surface without bacteria

Under SEM analysis, the samples of solid titani-

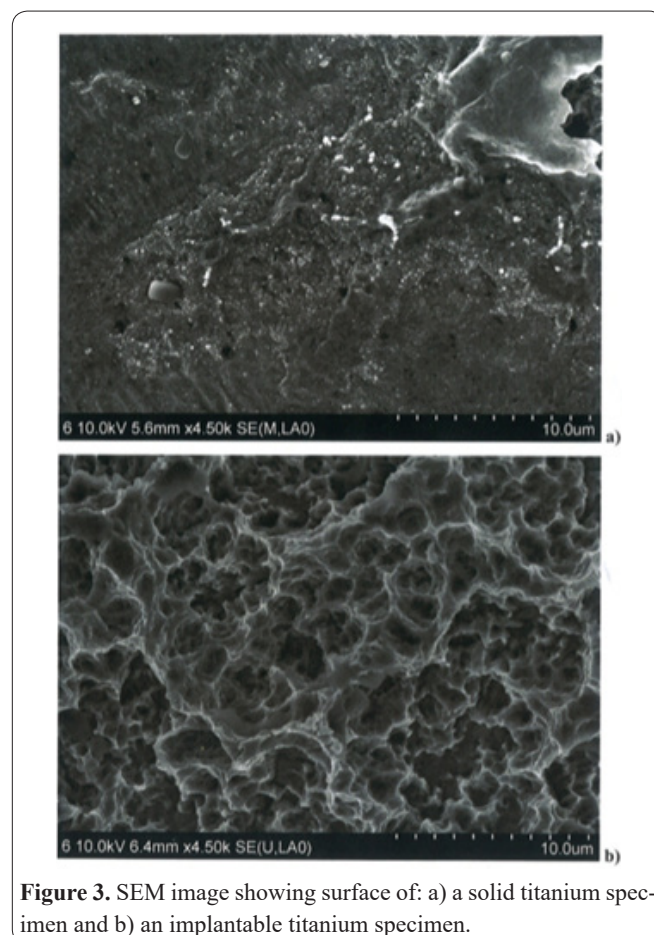


Figure 3. SEM image showing surface of: a) a solid titanium specimen and b) an implantable titanium specimen.

um presented an irregular surface that was relatively smooth (Figure 3a). The surface of the implantable titanium plates appeared different as it shows an array of micro-pits up to several microns in depth and of 3 to 5 μm in diameter (Figure 3b).

Raman spectroscopy analysis of the surface of implantable titanium specimens revealed the presence of a passivation layer of rutile-form crystallization (TiO_2). The width of the lines indicates the significant distribution of high concentrations of amorphous TiO_2 (Figure 4). This may facilitate bacterial adhesion due to the presence of a hydroxyl group on the surface that enables the formation of hydrogen bonds. However, adhesion of negatively charged bacteria could theoretically be impeded by the presence of negative charges on TiO_2 in $\text{pH} > 6$ solutions used in our experiments. Nevertheless, the proteins secreted by bacteria to form biofilms behave pI ranging from 3 to 10 allowing them to attach to materials of a high range of surface charges mainly through hydrophobic bonds that overcome ionic charges.

Characterization of the strains used

Optical microscopy of the *D. fairfieldensis* strain shows straight or curved bacilli measuring 0.5 to 1 μm in diameter and 2.5 to 5 μm in length (Figure 5), typical of the *Desulfovibrio* genus. Gram-stained smear of *D. desulfuricans* and *D. fairfieldensis* colonies was negative and revealed thin, curved-rod (comma) shaped bacilli that resemble the *Desulfovibrio* genus. Observation of one specimen in a fresh state revealed both bacillus strains to be highly mobile. Incubation of the *D. fairfieldensis* and *D. desulfuricans* strains in sulfate medium resulted in H_2S production and both strains produced desulfovirdin as assayed by the addition of 2 N NaOH. By examination at 365 nm, red fluorescence appeared indicating the release of the chromophore sirohydrochlorin by desulfovirdin. The catalase test, performed directly on the CBA culture medium, was positive for *D. fairfieldensis* bacterium and negative for *D. desulfuricans* strains. Finally, *D. fairfieldensis* and *D. desul-*

furicans were both found to be nonhemolytic on CBA culture medium. All of these characteristics strongly fit with those of the *Desulfovibrio* strains.

D. fairfieldensis and *D. desulfuricans* bacterial growth at 30 and 37°C

Daily absorbance measure at 600 nm enabled us to generate growth curves for *D. fairfieldensis* and *D. desulfuricans* at 30°C in DSMZ and AS medium. At 30°C, the exponential growth phase of the *D. desulfuricans* strain in DSMZ medium (Figure 6) appeared to occur between d 1 and 2, with maximum cell density obtained on d 10 ($A_{600} = 0.27$). After 10 days of incubation, absorbance decreased, potentially due to cell flocculation or bacterial lysis (Figure 6a). The growth rate constant, μ , is calculated during the observed exponential growth phase, which, in our conditions, was 0.371 d^{-1} or 0.015 h^{-1} , namely a generation time of approximately 45 h (Figure 6b).

For the *D. fairfieldensis* strain cultivated in the same conditions, the growth rate was significantly slower. Using the same method, and considering an exponential growth phase ranging from 1 to 11 d reaching an $A_{600\text{nm}} = 0.29$ (Figure 6a) and $\mu = 0.0786 \text{ d}^{-1}$ or 0.0033 h^{-1} , thus giving a generation time of approximately 212 h (Figure 6b).

At 37°C, the *D. fairfieldensis* strain, cultivated in DSMZ medium, presented exponential growth between d1 and d2 (Figure 6). Maximum cell density was reached on d4, where $A_{600\text{nm}} = 0.39$ or $8.2 \cdot 10^8$ bacteria/

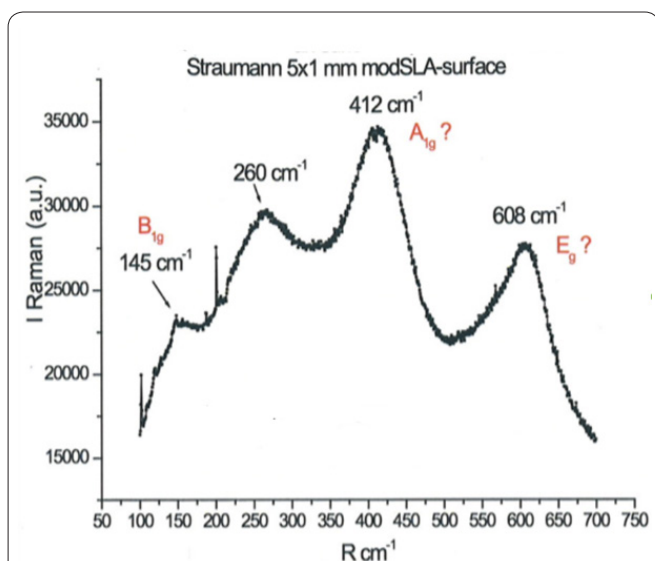


Figure 4. Raman spectroscopy of the surfaces of titanium dental implants indicating the presence of a passivation layer of TiO_2 . High proportions of this TiO_2 are probably amorphous due to the significant shift in wavelength of 154 cm^{-1} , 412 cm^{-1} and 608 cm^{-1} compared to the spectra of rutile-form pure titanium.

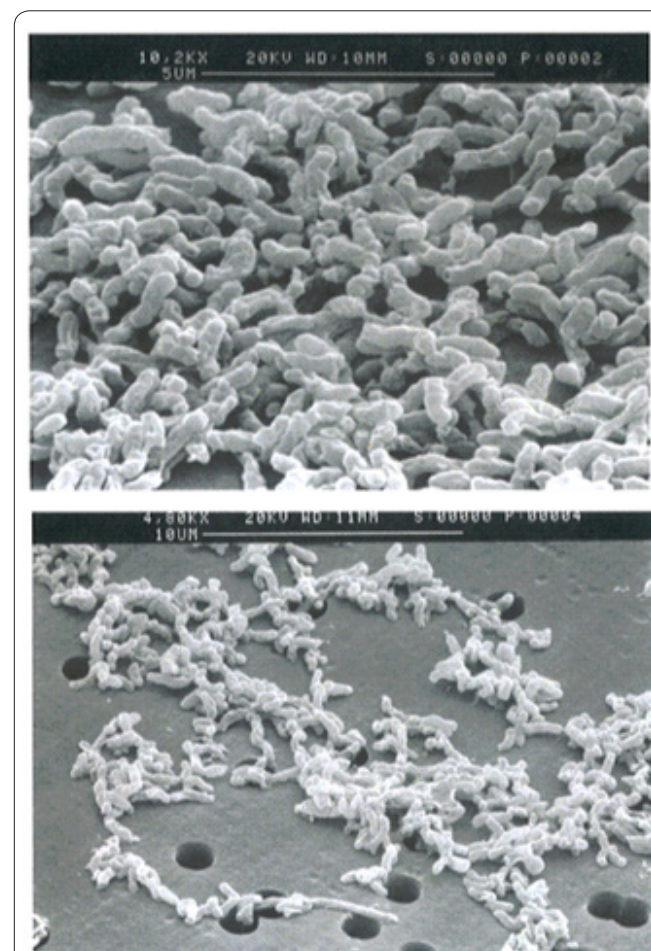


Figure 5. SEM imaging of *Desulfovibrio fairfieldensis* cells harvested from the filter membrane following 7 d of incubation in DSMZ medium.

mL. The μ constant was thus 0.476 d^{-1} (0.02 h^{-1}), giving a generation time of approximately 35 h (Figure 6b). In the artificial saliva medium (AS) at 37°C , the growth rate constant of *D. fairfieldensis* was 0.311 d^{-1} (0.013 h^{-1}) and the generation time was lower, around 53 h, indicating that growth was slightly decreased in artificial saliva (Figure 6b). Maximum bacterial growth was observed at d4 of incubation $A_{600\text{nm}} = 0.27$, namely $6.9 \cdot 10^8$ bacteria mL^{-1} (Figure 6a).

Both DSMZ and AS media enable the growth of both *Desulfovibrio* strains. Further assessment of growth in these two media at two different temperatures also clearly showed that *D. fairfieldensis* grows more slowly at 30°C than at 37°C , demonstrating a growth rate at the higher temperature equivalent to that of *D. desulfuricans* at 30°C .

D. fairfieldensis adhesion to titanium

Following culture, the bacterial cells were harvested and rinsed before being incubated in a KNO_3 solution with AS or DSMZ medium. The suspension was placed in contact with either solid titanium or implantable titanium. The incubation conditions are outlined in Table II.

Adhesion on solid or implantable titanium in KNO_3 medium

The adhesion test curve revealed that the number of cells adhered to the surface increased over time until presenting a plateau from 18 h of incubation onwards,

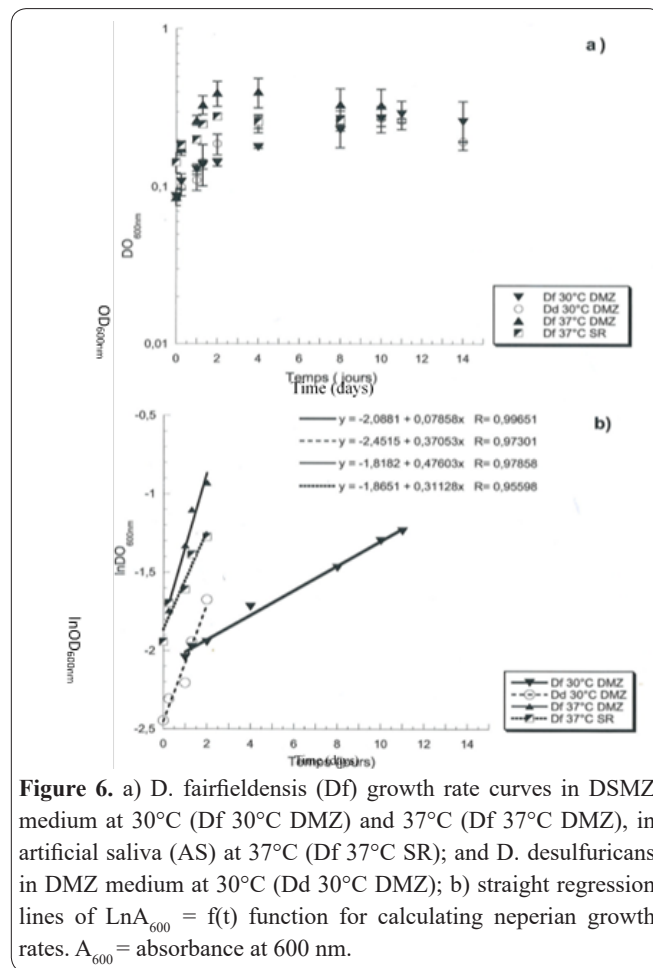


Figure 6. a) *D. fairfieldensis* (Df) growth rate curves in DSMZ medium at 30°C (Df 30°C DMZ) and 37°C (Df 37°C DMZ), in artificial saliva (AS) at 37°C (Df 37°C SR); and *D. desulfuricans* in DMZ medium at 30°C (Dd 30°C DMZ); b) straight regression lines of $\text{Ln}A_{600} = f(t)$ function for calculating neperian growth rates. A_{600} = absorbance at 600 nm.

Table 2. experimental condition for incubation of *D. fairfieldensis* suspensions in the presence of titanium specimens in KNO_3 or artificial saliva (AS) medium.

Dish N°	1	2	3	4	5	6
Df added	+	+	-	+	-	+
Medium	KNO_3 0.05 M	KNO_3 0.05 M	KNO_3 0.05 M	AS	AS	AS
Specimens/dish	0	5	2	5	2	0
pH t_0	7.0	7.0	7.0	7.0	7.0	7.0
0 h	T_{sT} Susp	$7 \cdot 10^8$	Nd		$< 10^{-4}$	
	T_{impT} Susp	$5.9 \cdot 10^8$		Nd	$< 10^{-4}$	
2 h	T_{sT}	Nd	$7.6 \cdot 10^5 \text{ b/cm}^2$			
	T_{impT}		$1.14 \cdot 10^6 \text{ b/cm}^2$	$3.4 \cdot 10^6$		
6 h	T_{sT}	Nd	$1.5 \cdot 10^6$			
	T_{impT}		$3.8 \cdot 10^6$	$2.2 \cdot 10^7$		
18 h	T_{sT} Susp	$7.1 \cdot 10^8$				
	T_{impT} Susp	$6.0 \cdot 10^8$	$3.55 \cdot 10^6$	$3.6 \cdot 10^7$		$6.8 \cdot 10^8$
48 h	T_{sT}		$2.1 \cdot 10^6$			
	T_{impT}		$3.8 \cdot 10^6$	$4.3 \cdot 10^7$		
96 h	T_{sT} Susp	$7.1 \cdot 10^8$	$2.1 \cdot 10^6$	$< 10^{-4}$		
	T_{impT} Susp	$6.0 \cdot 10^8$	$3.5 \cdot 10^6$	$< 10^{-4}$	$5.6 \cdot 10^7$	$< 10^{-4}$
pH t_{96}	6.7	6.7	6.7	7.0	7.0	7.0

The bacterial concentrations are also indicated, either in suspension in the solution (cel mL^{-1}) or on the specimen surface (cel cm^{-2}) according to incubation duration (0 h 96 h). Nd=not determined; T_{sT} : number of bacteria per cm^2 (b/cm^2) on solid titanium ; T_{impT} : number of bacteria per cm^2 (b/cm^2) on implantable titanium; Susp: Number of bacteria in 1 mL suspension (b/mL). Dishes 3 and 5 are abiotic controls.

at which point the maximum number of attached bacteria was approximately 2.10^6 bacteria/cm² (Figure 7a). We present herein only one representative test for solid titanium at 30°C. This test enabled us to better adapt our incubation conditions (cell concentrations in suspension) and determine the best timepoints for sampling as we had hypothesized that the behaviour of the bacterial cells towards the implantable titanium would be similar to that towards solid titanium. We thus used the same concentration of cells ($5.9.10^8$ cells/mL) and applied the same timepoints for studying adhesion on the implantable titanium specimens. The adhesion curve produced was quite similar to that obtained with solid titanium, namely with an adhesion phase occurring over the first 18 h followed by a plateau. The adhesion kinetics were slightly higher with the implantable titanium: 6.10^5 versus 2.10^5 cells cm⁻² h⁻¹ and the maximum number of attached cells was also higher at the plateau: 4.10^6 versus 2.10^6 cells cm⁻² h⁻¹ (Figure 7a), probably due to the implantable titanium that behave a rougher surface thus facilitating cell adherence and an increased surface area. Taking into account the level of uncertainty of our tests on implantable titanium, as well as the lack of solid titanium replicate, those results should nevertheless be interpreted with care. As for the control bacterial suspension in KNO₃ medium without titanium, no significant variation in the number of bacteria was observed during the 96 h-incubation period due to the absence of nutrients in that medium (Table II). Consequently, we can assume that the increase in cell numbers observed in the first 18 h of incubation was indeed due to cell adhesion and not a result of the multiplication of already attached bacteria. Furthermore, the controls (dishes #3 and #5, unexposed to bacteria) did not reveal any bacteria on the surface of the titanium specimens, neither at 0, 18 nor 96 h, (Table II), attesting that the experiments were conducted in adequately aseptic conditions. It is noteworthy that, during incubation, pH only slightly decreased, from 7.0 to 6.7, which likely has no major impact on cell adhesion (Table II).

Adhesion on implantable titanium in artificial saliva

In AS medium, the adhesion kinetics of *D. Fairfieldensis* on titanium is solved in two phases: one of rapid accumulation lasting from 0 to 6 h, resulting in a final load of 4.6×10^6 cells cm⁻² h⁻¹; and a slow accumulation phase ranging from 18 to 96 h with a final load of $2.35.10^6$ cells cm⁻² h⁻¹ (Figure 7b). In contrast to the KNO₃ medium, AS ones enable bacterial growth (0.013 h⁻¹ at 37°C), following their adhesion, as evidenced by a higher adhesion rate and final number of fixed bacteria (one decimal log more fixed bacteria, Table II). The observed consistent increase of cell number beyond the first 18 h of incubation rather than the pseudo-plateau observed with KNO₃ medium is likely the result of the growth of bacteria on titanium specimen. Noteworthy it should be noted that the increase rate is linear what perhaps may be due to nutrient depletion in the medium (Figure 6a). Finally, the ion composition of AS which ionic strength is equivalent to 0.23 M NaCl could contribute to favour the adhesion of bacteria to the TiO₂ surface.

One can assume that bacteria are the cylindrical object of $0.5 \mu\text{m} \times 2 \mu\text{m}$, forming a surface of $0.946 \mu\text{m}^2$ namely around $1 \mu\text{m}^2$ (Figure 5). As the final load was

$5.63.10^7$ cells cm⁻² for a 96 h-incubation period in AS buffer, the maximum colonized surface is 0.563 cm^2 namely 56 % of the upper surface area of the used titanium specimen. Considering the 5 specimens of dish#4 titanium, an adhesion of 0.55 % of $2.8.10^{10}$ cells in suspension (7.10^8 cells/mL x 40 mL) is equal to $1.55.10^8$ bacteria.

Demonstration of biofilm formation

Following a 30 d-incubation period in DSMZ me-

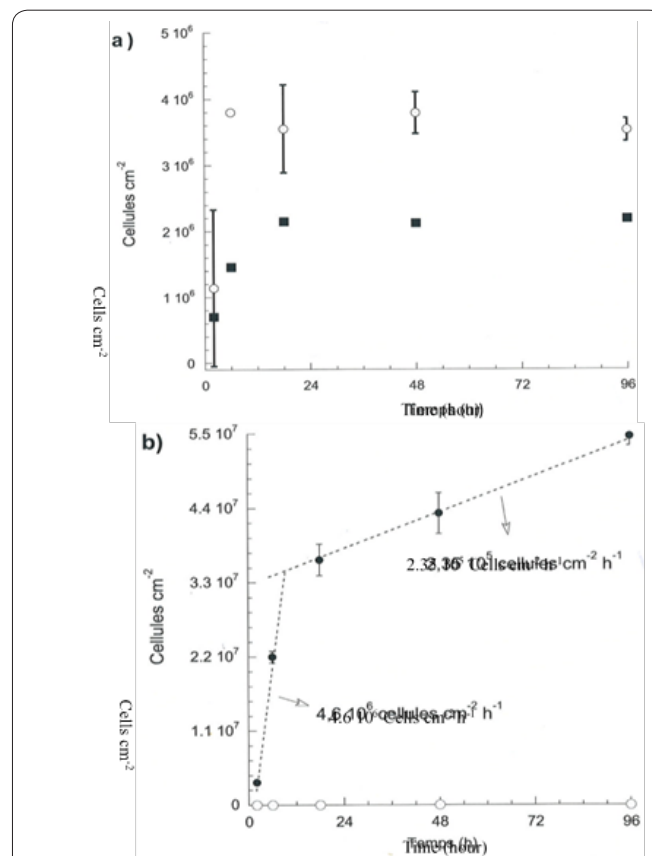


Figure 7. adhesion of *D. fairfieldensis* according to incubation duration: a) in 0.05 M KNO₃ medium at 30°C on solid titanium (black squares n=1) or on implantable titanium (white circles, n=3); b) in artificial saliva (AS) medium on implantable titanium, at 37°C (black circles, n=3). The abiotic control at 37°C (no cells added) is represented by white circles. The two values marked by arrows are the adhesion rates, as the adhesion kinetics is biphasic.

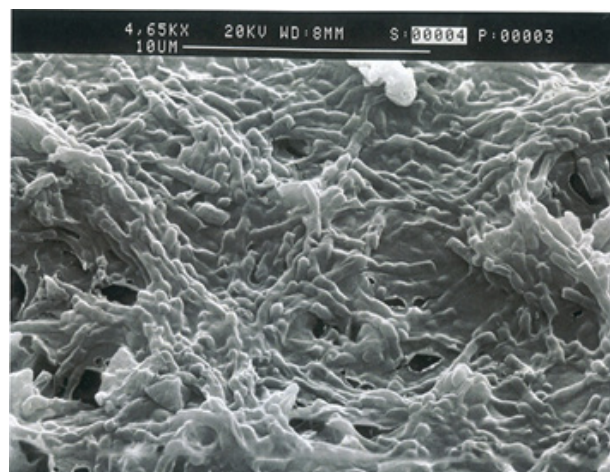


Figure 8. SEM imaging demonstrating a biofilm of *D. fairfieldensis* on the surface of an implantable titanium specimen in DSMZ medium incubated at 37°C, 30 days after incubation in vials.

dium at 37°C and pH = 7.8 in sealed vials to avoid the medium evaporation, very dense aggregates were observed with SEM over the entire surface (Figure 8). These aggregates presented as typical biofilms, namely bacterial cells embedded in a polymeric matrix attached to the specimen surface. These accumulations were located at crevices and pits onto the titanium rough surface, designing microscopic “spider webs”. The bacteria appeared to have multiplied and produced these extracellular polymeric substances that formed a matrix of dense fibres clearly visible on SEM (Figure 8). Note that no similar polymeric matrix was observed on SEM for the cells in suspension without titanium specimens (Figure 5).

Discussion

This study sought to evaluate the adhesion capacity of *Desulfovibrio fairfieldensis* bacteria, along with their ability to form biofilm. We monitored the adhesion of these bacteria on 2 titanium materials in 3 media, then investigated samples for the formation of biofilms following long incubation (30 d).

Growth of *D. fairfieldensis* and *D. desulfuricans* in the chosen media

Sulfate-reducing bacteria require an anaerobic environment to grow, and their growth is relatively slow in anaerobic chambers even in nutrient-rich media. The stationary phase is generally only reached after 4 to 10 d, depending on the incubation conditions and the strain. This growth is further hampered, at least in part, by the production of toxic H₂S that accumulates in the medium (24).

The most thoroughly studied species of the genus is *D. desulfuricans*. The specific growth rates (μ) we obtained in our hand at 30°C (0.015 h⁻¹ in DSMZ; DSM #642 strain, equivalent to ATCC #29577) were in line with those obtained by previous authors. Lopes *et al.* (22), for example, tested Postgate C medium, also using anaerobic conditions, and obtained a μ value of 0.023 h⁻¹ for the same strain at 26°C, showing a maximum cell density of 1.2.10⁹ bacteria/mL at 60 h of culture. Other studies on *D. desulfuricans* (ATCC #5575) have reported values 10 times higher in Postgate G medium at 35°C and (24). We did not obtain such values with *D. fairfieldensis* ATCC #700045, even at 37°C as the highest μ value was 0.02 h⁻¹. The absence of precise data on the growth kinetics of this strain makes we unable to compare our results with those of the literature.

Bacterial adhesion and growth of adhered bacteria

In 0.05 M KNO₃ medium, *D. fairfieldensis* adhesion is relatively fast and a plateau was reached after 18 h, on both solid titanium and implantable titanium, at which point the bacteria number was respectively 2.10⁶ and 3.5.10⁶ bacteria/cm². Cell plateau was also reported by Hjelm *et al.* (25) following similar incubation times of *Shewanella putrefaciens*, using a stainless steel specimen and similar PBS buffer without nutrient, yet with.

In KNO₃ 0.05 M medium, bacterial adhesion occurs rapidly on titanium surfaces and reaches equilibrium on both native and implantable titanium specimens of 10⁶ bacteria/cm². Lopes *et al.* (22) and Hjelm *et al.* (25) re-

port similar values of attached bacteria on stainless steel with *D. desulfuricans* and *S. putrefaciens* respectively. In their study of *Streptococcus sanguis* and *S. constellatus*, Mabboux *et al.* (26) reported a number of adhering bacteria on polished titanium varying from 2 to 4.10⁶ cm⁻². *D. fairfieldensis* thus adheres with high efficiency to titanium in a non-nutrient medium; this adhesion shows a sufficient strength to not come detached by saline solution washing suggesting that it is not driven by ionic forces or hydrogen bonds rather by hydrophobic forces. Noteworthy *D. fairfieldensis* displays at least equal adhesion efficiency to that of other bacteria tested in the literature, regardless of the experimental differences inherent to each study.

In AS medium, adhesion was found to be much more significant (5.6.10⁷ bacteria/cm⁻²) than that achieved in KNO₃. KNO₃ medium does not enable bacterial growth, and thus allows us to make difference in bacteria that adhere and the growth and bacteria already adhering to the surface. Thus, the results suggest there are two phases during bacterial adhesion: the first consisting of a constant adhesion rate, and the second observed solely in nutrient-rich media when the number of attached bacteria slightly increases after the 18-h timepoint, attributed to the growth of bacteria already adhering to the surface.

The faster kinetics of bacterial adhesion observed with specimens of implantable titanium (6.10⁵ bacteria h⁻¹cm⁻² in KNO₃ medium) compared to that obtained on solid titanium (2.10⁵ bacteria h⁻¹cm⁻²) could be due to the surface roughness. The titanium used for implants features a much rougher surface, that should facilitate effective osseointegration and also adhesion and colonization of bacterial cells, which are of a similar size to, if not smaller than, the porous texture of the solid titanium. This is in line with the results of a previous study (27), which reported that the smoother the surface of the titanium is, the fewer *Porphyromonas gingivalis* can adhere. A compromise between a surface that enables osseointegration with sufficient roughness that facilitates the adhesion of osteoblasts and limiting bacterial adhesion must therefore be found. If we are then to extrapolate these values to *in situ* adhesion, we must also determine the exact nature of the implant surface. First of all, it is more pertinent to consider adhesion onto TiO₂ rather than onto Ti since the analysis of surfaces performed in our study has demonstrated the presence of a rutile-form passivation layer. Secondly, as soon as the metal is implanted, it is likely that the surface is also modified by a conditioned layer of ions and proteins from the implant surrounding space and reacting with it. With this in mind, we opted to experiment with so-called “artificial” saliva, yet we did not take into account the role of saliva proteins on *D. fairfieldensis* adhesion, as these are not present in the AS medium we used. The pre-eminent role these types of proteins play in bacterial adhesion (26) and growth (28) is well known, and it would thus be interesting to study their effect on adhesion to titanium. Such protein fixation on TiO₂ nanoparticles was shown for 2 decades: virtually all NP in physiologic media are surrounded by a protein crown of highly different physico-chemical parameters (function, molecular mass and pI). The protein part is called “corona” and participates certainly in the fate of NP in the hu-

man body as they will participate in the fate of implants (29). Thus *D. fairfieldensis* is certainly surrounded by proteins issued from culture medium or from bacteria secretion that are involved to implant adhesion.

Nevertheless, there is limited contact between saliva and the implant surface. The liquid that actually surrounds the implant is instead gingiva fluid, an inflammatory exudate with a similar composition to lymph serum: enzymes, plasma proteins and immunological proteins (28). Given this, it would be pertinent to study bacterial adhesion and biofilm formation in this gingiva fluid rather than in saliva and also to determine by mass spectrometer the composition of the biofilm proteins as it was already performed with TiO₂ nanoparticles (29).

Biofilm formation

In order to observe the formation of biofilm on the surface of implantable titanium, we incubated a bacterial suspension with implant specimens in a nutrient-rich DSMZ medium, allowing us to observe the bacteria's strongest growth. After 30 d, biofilms of accumulated bacteria within a polymeric matrix were clearly visible on SEM.

This observation demonstrates, for the first time to the best of our knowledge, *D. fairfieldensis* bacteria's capacity to form biofilm-like other bacteria. The polymeric matrix observed could without any doubt strengthen the bacteria's resistance to different host defences: phagocytes, lysozyme, IgA from saliva and antibiotics and biocides. The formation of biofilm is then likely to cause destruction to epithelial tissue and connective fibres through production of H₂S, which should facilitate bacteria penetration during the osseointegration process following the implantation that may cause periodontal infections and decrease implant longevity.

We demonstrated the adhesion ability of *D. fairfieldensis* to titanium native and implantable implants, as well as biofilm formation. However, further study is necessary to strengthen our preliminary results as understanding the: (i) behaviour of *D. fairfieldensis* on polished specimens (ii) biofilm formation, both in artificial saliva and natural saliva, (iii) adhesion mechanism by determining which protein of the medium or secreted by the bacteria are involved and (iv) role of surface free energy, roughness, hydrophobicity of processed titanium in bacterial adhesion.

The clinical interest of this study lies in the guarantee that, with the results of these further works, we should be able to propose modifications of implant surfaces or implantation methods that will prevent bacterial adhesion and avoid corrosion while simultaneously facilitate colonization of bone cells.

One alternative is to research materials defined as being "antiadhesive", an ambitious goal that continues to be explored, for there are potential applications in a vast array of medical and even industrial fields. Zirconia (ZnO₂) materials are occasionally announced as candidates for this alternative, one the one hand due to their mechanical and esthetic properties fulfilling the needs of dental implantology, and on the other hand due to studies have shown that bacterial adhesion to these materials in an oral environment is less effective compared to titanium (30). Still, the difference in bacterial adhesion between these materials is slight, and only dem-

onstrated over short incubation durations (≤ 24 h), thus not representative of the real-time needed for biofilm to form on a surface.

This is the first time the *D. fairfieldensis* ability to grow in the presence of titanium of a dental implant quality and to form biofilms has been demonstrated. Embedded in this biofilm, this strain is probably kept safer from attacks from its environment. If we are to limit its growth, our study has focused on the nature of the surface in bacterial growth and adhesion as well as the nature of the media used. In order to ensure osseointegration, an implant needs a significant level of roughness for attracting osteoblasts and hydroxyapatite formation and limiting the adhesion ability of bacteria.

Acknowledgements

The work presented in this document was carried out within the framework of the IMPLANT operation (Positive Medical Personalised innovANTs implanTables) co-financed by the European Union through the ERDF-ESF Operational "Programme Lorraine et Massif des Vosges 2014-2020".

The authors are indebted to Sinan Kamagate (LCPME, UMR #7564 CNRS, Université de Lorraine) for its technical contributions and its immense contribution to bacteriology studies, to Sébastien Crémel (LCPME) for Raman spectroscopy and Luc Marchal (Core Imaging, School of Medicine) for SEM studies. The authors also thank Lozniewski Alain for its help in bacteriology studies and Bertrand H Rihn for manuscript revision as well as the members of the microbiology team of the laboratory of physical chemistry and microbiology for the environment (LCPME).

References

1. Brånemark PI, Hansson BO, Adell R, Breine U, Lindström J, Hallén O, et al. Osseointegrated implants in the treatment of the edentulous jaw. Experience from a 10-year period. *Scand J Plast Reconstr Surg Suppl.* 1977;16:1–132.
2. Adell R, Lekholm U, Rockler B, Brånemark P-I. A 15-year study of osseointegrated implants in the treatment of the edentulous jaw. *Int J Oral Surg.* 1981 Jan 1;10(6):387–416.
3. Zarb GA, Alberktsson T. [Criteria for determining clinical success with osseointegrated dental implants]. *Cah Prothese.* 1990 Sep;(71):19–26.
4. Schmidt R. Comportement des matériaux dans les milieux biologiques: applications en médecine et biotechnologie. Presses Polytechniques et Universitaires Romandes, Lausanne, Switzerland. 1999. *Traité Des Matériaux*, pp. 166–173.
5. Marchal A., Rapin C., Jacquot B., Steinmetz P. Étude de la corrosion d'alliages orthodontiques en milieu salivaire. Comportement en couplage galvanique. In: *Actual Odontol.* Ed. Romillat. 2002. p. 461–70.
6. Rao TS, Kora AJ, Anupkumar B, Narasimhan SV, Feser R. Pitting corrosion of titanium by a freshwater strain of sulphate reducing bacteria (*Desulfovibrio vulgaris*). *Corros Sci.* 2005 May 1;47(5):1071–84.
7. Tee W, Dyal-Smith M, Woods W, Eisen D. Probable new species of *Desulfovibrio* isolated from a pyogenic liver abscess. *J Clin Microbiol.* 1996 Jul 1;34(7):1760–4.
8. Warren YA, Citron DM, Merriam CV, Goldstein EJC. Biochemical Differentiation and Comparison of *Desulfovibrio* Species and Other Phenotypically Similar Genera. *J Clin Microbiol.* 2005 Aug

1;43(8):4041–5.

9. Langendijk PS, Kulik EM, Sandmeier H, Meyer J, van der Hoeven JS. Isolation of *Desulfomicrobium orale* sp. Nov. and *Desulfovibrio* strain NY682, oral sulfate-reducing bacteria involved in human periodontal disease. *Int J Syst Evol Microbiol.* 2001;51(3):1035–44.

10. Loubinoux J, Bisson-Boutelliez C, Miller N, Faou AEL. Isolation of the provisionally named *Desulfovibrio fairfieldensis* from human periodontal pockets. *Oral Microbiol Immunol.* 2002;17(5):321–3.

11. Goldstein EJC, Citron DM, Peraino VA, Cross SA. *Desulfovibrio desulfuricans* Bacteremia and Review of Human *Desulfovibrio* Infections. *J Clin Microbiol.* 2003 Jun;41(6):2752.

12. Dupont-Morrall I. Les bactéries sulfato-réductrices et la corrosion bactérienne. *Bull Soc Fr Microbiol.* 2004;108–15.

13. Zhu XY, Lubeck J, Kilbane JJ. Characterization of Microbial Communities in Gas Industry Pipelines. *Appl Environ Microbiol.* 2003 Sep 1;69(9):5354–63.

14. Muthukumar N, Rajasekar A, Ponmariappan S, Mohanan S, Maruthamuthu S, Muralidharan S, et al. Microbiologically influenced corrosion in petroleum product pipelines – A review. *IJEB Vol4109* Sept 2003 [Internet]. 2003 Sep [cited 2019 Nov 14]; Available from: <http://nopr.niscair.res.in/handle/123456789/17162>

15. Moreno DA, Cano E, Ibars JR, Polo JL, Montero F, Bastidas JM. Initial stages of microbiologically influenced tarnishing on titanium after 20 months of immersion in freshwater. *Appl Microbiol Biotechnol.* 2004 May 1;64(4):593–8.

16. Loubinoux J, Jaulhac B, Piemont Y, Monteil H, Faou AEL. Isolation of Sulfate-Reducing Bacteria from Human Thoracoabdominal Pus. *J Clin Microbiol.* 2003 Mar 1;41(3):1304–6.

17. Loubinoux J, Mory F, Pereira IAC, Faou AEL. Bacteremia Caused by a Strain of *Desulfovibrio* Related to the Provisionally Named *Desulfovibrio fairfieldensis*. *J Clin Microbiol.* 2000 Feb 1;38(2):931–4.

18. McDougall R, Robson J, Paterson D, Tee W. Bacteremia caused by a recently described novel *Desulfovibrio* species. *J Clin Microbiol.* 1997 Jul 1;35(7):1805–8.

19. Scola BL, Raoult D. Third Human Isolate of a *Desulfovibrio* sp. Identical to the Provisionally Named *Desulfovibrio fairfieldensis*. *J Clin Microbiol.* 1999 Sep 1;37(9):3076–7.

20. Loubinoux J, Valente FMA, Pereira IAC, Costa A, Grimont PAD, Le Faou AE. Reclassification of the only species of the genus *Desulfomonas*, *Desulfomonas pigra*, as *Desulfovibrio piger* comb. Nov. *Int J Syst Evol Microbiol.* 2002;52(4):1305–8.

21. Sheng X, Ting YP, Pehkonen SO. Force measurements of bacterial adhesion on metals using a cell probe atomic force microscope. *J Colloid Interface Sci.* 2007 Jun 15;310(2):661–9.

22. Lopes FA, Morin P, Oliveira R, Melo LF. The influence of nickel on the adhesion ability of *Desulfovibrio desulfuricans*. *Colloids Surf B Biointerfaces.* 2005 Dec 10;46(2):127–33.

23. Creml S. Contribution à l'étude des interactions ions-surfaces: application aux systèmes Se(IV), Se(VI), U(VI) sur TiO₂ rutile et Eu(III) sur dickite [Internet]. 09 [cited 2019 Nov 14]. Available from: <http://www.theses.fr/2007NAN10085/document>

24. Okabe S, Nielsen PH, Jones WL, Characklis WG. Sulfide product inhibition of *Desulfovibrio desulfuricans* in batch and continuous cultures. *Water Res.* 1995 Feb 1;29(2):571–8.

25. Hjelm M, Hilbert LR, Møller P, Gram L. Comparison of adhesion of the food spoilage bacterium *Shewanella putrefaciens* to stainless steel and silver surfaces. *J Appl Microbiol.* 2002;92(5):903–11.

26. Mabboux F, Ponsonnet L, Morrier J-J, Jaffrezic N, Barsotti O. Surface free energy and bacterial retention to saliva-coated dental implant materials—an in vitro study. *Colloids Surf B Biointerfaces.* 2004 Dec 25;39(4):199–205.

27. Pier-Francesco A, Adams RJ, Waters MGJ, Williams DW. Titanium surface modification and its effect on the adherence of *Porphyromonas gingivalis*: an in vitro study. *Clin Oral Implants Res.* 2006;17(6):633–7.

28. Darveau RP, Tanner A, Page RC. The microbial challenge in periodontitis. *Periodontol 2000.* 1997;14(1):12–32.

29. Joubert O, Rihn P and Rihn BH. The nanoparticle “coronome” is mainly explained by Interpro domains of proteins. 113-131 pp. In *Biomedical applications of nanoparticles*. 328 pp. Editor BH Rihn. CRC Press, New York, 2017.

30. Scarano A, Piattelli M, Caputi S, Favero GA, Piattelli A. Bacterial Adhesion on Commercially Pure Titanium and Zirconium Oxide Disks: An In Vivo Human Study. *J Periodontol.* 2004;75(2):292–6.